blood

American Society of Hematology
2021 L Street NW, Suite 900,
Washington, DC 20036
Phone: 202-776-0544 | Fax 202-776-0545
editorial@hematology.org

Aberrant single-cell phenotype and clinical implications of genotypically-defined polyclonal plasma cells in myeloma

Tracking no: BLD-2024-025643R1

Matteo Claudio Da Viá (Fondazione IRCCS Ca' Granda Ospedale Maggiore Policlinico, Italy) Francesca Lazzaroni (Fondazione IRCCS Ca' Granda Ospedale Maggiore Policlinico, Italy) Antonio Matera (University of Milan, Italy) Alessio Marella (University of Milan, Italy) Akihiro Maeda (Fondazione IRCCS Ca' Granda Ospedale Maggiore Policlinico, Italy) Claudio De Magistris (Fondazione IRCCS Ca' Granda Ospedale Maggiore Policlinico, Italy) Loredana Pettine (FONDAZIONE IRCCS CA' GRANDA OSPEDALE MAGGIORE POLICLINICO, Italy) Antonio Solimando (University of Bari Medical School, Italy) Vanessa Desantis (University of Bari Medical School, Italy) Giuseppe Peretti (Department of Biomedical Sciences for Health, University of Milan, Milan, Italy, Italy) Laura Mangiavini (Department of Biomedical Sciences for Health, University of Milan, Milan, Italy, Italy) Riccardo Giorgino (IRCCS Istituto Ortopedico Galeazzi, Italy) Sonia Fabris (Fondazione IRCCS Ca' Granda Ospedale Maggiore Policlinico, Italy) Stefania Pioggia (Fondazione IRCCS Ca' Granda Ospedale Maggiore Policlinico, Italy) Alfredo Marchetti (Fondazione IRCCS Ca' Granda Ospedale Maggiore Policlinico, Italy) Marzia Barbieri (IRCCS Ospedale Maggiore Policlinico, Italy) Silvia Lonati (University of Milan, Italy) Alessandra Cattaneo (Fondazione IRCCS Ca' Granda Ospedale Maggiore Policlinico , Milan, Italy) Marta Tornese (Fondazione IRCCS Ca' Granda Ospedale Maggiore Policlinico, SC Patologia Clinica, Flow Cytometry Laboratory, Milan, Italy, Italy) Margherita Scopetti (Fondazione IRCCS Ca' Granda Ospedale Maggiore Policlinico, Italy) Emanuele Calvi (University of Milan, Italy) Nayyer Latifinavid (University of Milan, Italy) Giancarlo Castellano (Fondazione IRCCS Ca' Granda Ospedale Maggiore Policlinico, Italy) Federica Torricelli (Azienda USL-IRCCS di Reggio Emilia, Italy) Antonino Neri (Azienda USL-IRCCS di Reggio Emilia, Reggio Emilia, Italy, Italy) Cathelijne Fokkema (Erasmus MC Cancer Institute, Netherlands) Tom Cupedo (Erasmus University Medical Center, Netherlands) Marta Lionetti (University of Milan, Italy) Francesco Passamonti (2 Department of Oncology and Hemato-Oncology, University of Milan, 20122 Milan, Italy, Italy) Niccolo Bolli (Hematology Unit, Fondazione IRCCS Ca' Granda Ospedale Maggiore Policlinico, 20122 Milan, Italy, Italy)

Abstract:
Multiple Myeloma is driven by clonal plasma cell (cPC)-intrinsic factors and changes in the tumorigenic microenvironment (TME). To investigate if residual polyclonal PCs (pPCs) are disrupted, single-cell (sc) RNAseq and sc B-cell receptor analysis were applied in a cohort of 46 samples with PC dyscrasias and 21 healthy donors (HDs). Out of n=234,789 PCs, 64,432 were genotypically identified as pPCs with frequencies decreasing over different disease stages, from 23.66% in monoclonal gammopathy of undetermined significance (MGUS) to 3.23% in MMs (p=0.00012). Both cPCs and pPCs had a comparable expression of typical lineage markers (i.e. CD38, CD138), while others were more variable (CD27, ITGB7). Only cPCs overexpressed oncogenes (e.g. CCND1/2, NSD2), but CCND3 was often expressed in pPCs. BCMA was expressed on both p- and cPCs, while GPRC5D was mostly upregulated in cPCs with implications for on-target, off-tumor activity of targeted immunotherapies. In comparison with HDs, pPCs from patients showed upregulated autophagy and disrupted interaction with TME. Importantly, interferon related pathways where significantly enriched in pPCs from patients vs HDs (p-adjusted < 0.05) showing an inflamed phenotype affecting genotypically normal PCs. Function of pPCs was consequently impacted and correlated with immunoparesis, driven by disrupted cellular interactions with TME. Leveraging our scRNAseq data, we derived a “healthy PC signature” that could be applied to bulk transcriptomics from the CoMMpass dataset and predicted significantly better PFS and OS (log rank p < 0.05 for both). Our findings show that genotypic, single-cell identification of pPCs in PC dyscrasias has relevant pathogenic and clinical implications.

Conflict of interest: COI declared - see note

COI notes: N.B. received honoraria for Amgen, GSK, Janssen, Jazz, Pfizer, Takeda. M.C.D.V. served as Advisory Board for Takeda, Menarini, Amgen, Pfizer, Johnson & Johnson, and on Speakers Bureau for Johnson & Johnson, Sanofi and GSK. F.P. received honoraria during the last two years for lectures from Novartis, Bristol-Myers Squibb, Abbvie, GSK, Janssen, AOP Orphan and for advisory boards from Novartis, Bristol-Myers Squibb/ Celgene, GSK, Abbvie, AOP Orphan, Janssen, Karyiopharma, Kyowa Kirin and MEI, Sumitomo, Kartos. The remaining Authors declare no competing financial interest. AGS has received speaker honoraria from Sanofi, Amgen, and AstraZeneca. He has also participated in advisory boards for Pfizer and Menarini and received travel support for educational purposes from Janssen-Cilag.

Preprint server: Yes; bioRxiv 10.1101/2024.05.26.595470

Author contributions and disclosures: N.B., M.C.D.V. F.L., conceived the project; N.B., M.C.D.V., F.L., designed the experiments; N.B., M.C.D.V., C.D.M, L.P., enrolled and followed up patients and acquired data; M.C.D.V., F.L., A.M., A.M., performed single cell experiments; A.M. verified the raw data before analyses and performed pre-processing bioinformatic analysis; M.C.D.V., F.L., A.M., performed the bioinformatic analysis and interpreted data; M.L., S.P., S.F., E.C., S.L., M.S., N. L., G. C., A.G.S., V.D.S., G.M.P., L.M., R.G., A.N., F.T., K.F., T.C., F.P., contributed with scientific discussions; A.C., M.T., performed the flow cytometry experiments; N.B., F.L., A.M., M.C.D.V., wrote the manuscript, which has been revised by all the authors.

Non-author contributions and disclosures: No;

Agreement to Share Publication-Related Data and Data Sharing Statement: Further information and requests should be directed and will be fulfilled by the lead contact, Niccolò Bolli (niccolo.bolli@unimi.it). The raw data, have been deposited at the European Genome-Phenome Archive (https://ega-archive.org/) under accession numbers EGAC50000000232. R scripts are available on https://gitlab.com/bollilab.

Clinical trial registration information (if any):

Aberrant single-cell phenotype and clinical implications of genotypically-defined polyclonal plasma cells in myeloma

Authors

Matteo Claudio Da Vià[1*], Francesca Lazzaroni[1*], Antonio Matera[2], Alessio Marella[2], Akihiro Maeda[1], Claudio De Magistris[1], Loredana Pettine[1], Antonio Giovanni Solimando[3], Vanessa Desantis[4], Giuseppe M. Peretti[5,6], Laura Mangiavini[5,6], Riccardo Giorgino[5], Sonia Fabris[1], Stefania Pioggia[1], Alfredo Marchetti[1], Marzia Barbieri[1], Silvia Lonati[2], Alessandra Cattaneo[7], Marta Tornese[7], Margherita Scopetti[1], Emanuele Calvi[2], Nayyer Latifinavid[2], Giancarlo Castellano[1], Federica Torricelli[8], Antonino Neri[9], Cathelijne Fokkema[10], Tom Cupedo[10], Marta Lionetti[2], Francesco Passamonti[1,2], Niccolò Bolli[1,2#]

Affiliations

[1] Hematology Unit, Fondazione IRCCS Ca' Granda Ospedale Maggiore Policlinico, 20122 Milan, Italy.
[2] Department of Oncology and Hemato-Oncology, University of Milan, 20122 Milan, Italy.
[3] Department of Precision and Regenerative Medicine and Ionian Area (DiMePRe-J), Unit of Internal Medicine "Guido Baccelli", University of Bari "Aldo Moro" Medical School, Bari, Italy.
[4] Department of Precision and Regenerative Medicine and Ionian Area (DiMePRe-J), Section of Pharmacology, University of Bari "Aldo Moro" Medical School, Bari, Italy.
[5] IRCCS Istituto Ortopedico Galeazzi, Milan, Italy
[6] Department of Biomedical Sciences for Health, University of Milan, Milan, Italy
[7] Flow Cytometry Laboratory, Clinical Pathology Unit, IRCCS Foundation Ca' Granda Ospedale Maggiore Policlinico, Milan, Italy.
[8] Laboratory of Translational Research, Azienda USL-IRCCS di Reggio Emilia, 42123 Reggio Emilia, Italy.
[9] Scientific Directorate, Azienda USL-IRCCS di Reggio Emilia, 42123 Reggio Emilia, Italy.
[10] Department of Hematology, Erasmus MC Cancer Institute, Erasmus Medical Center, Rotterdam, the Netherlands.

* These authors contributed equally to this work
[#] Corresponding author

Correspondence to: Niccolò Bolli, Hematology Unit, Fondazione IRCCS Cà Granda Ospedale Maggiore Policlinico, Via Francesco Sforza 35, 20122, Milan, Italy. niccolo.bolli@unimi.it ; +390255033334

RESOURCE AVAILABILITY

Further information and requests should be directed and will be fulfilled by the lead contact, Niccolò Bolli (niccolo.bolli@unimi.it). The raw data, have been deposited at the European Genome-Phenome Archive (https://ega-archive.org/) under accession numbers EGAC50000000232. R scripts are available on https://gitlab.com/bollilab.

KEY POINTS

1. scRNA-seq analysis of polyclonal PCs in patients shows an inflammatory phenotype that correlates with myeloma pathogenesis
2. Inflamed polyclonal PCs have perturbed interactions with the TME leading to immunoparesis and correlate with decreased survival in MM

SUMMARY

Multiple Myeloma is driven by clonal plasma cell (cPC)-intrinsic factors and changes in the tumorigenic microenvironment (TME). To investigate if residual polyclonal PCs (pPCs) are disrupted, single-cell (sc) RNAseq and sc B-cell receptor analysis were applied in a cohort of 46 samples with PC dyscrasias and 21 healthy donors (HDs). Out of n=*234,789* PCs, 64,432 were genotypically identified as pPCs with frequencies decreasing over different disease stages, from 23.66% in monoclonal gammopathy of undetermined significance (MGUS) to 3.23% in MMs (p=0.00012). Both cPCs and pPCs had a comparable expression of typical lineage markers (i.e. CD38, CD138), while others were more variable (CD27, ITGB7). Only cPCs overexpressed oncogenes (e.g. CCND1/2, NSD2), but CCND3 was often expressed in pPCs. BCMA was expressed on both p- and cPCs, while GPRC5D was mostly upregulated in cPCs with implications for on-target, off-tumor activity of targeted immunotherapies. In comparison with HDs, pPCs from patients showed upregulated autophagy and disrupted interaction with TME. Importantly, interferon related pathways where significantly enriched in pPCs from patients vs HDs (p-adjusted < 0.05) showing an inflamed phenotype affecting genotypically normal PCs. Function of pPCs was consequently impacted and correlated with immunoparesis, driven by disrupted cellular interactions with TME. Leveraging our scRNAseq data, we derived a "healthy PC signature" that could be applied to bulk transcriptomics from the CoMMpass dataset and predicted significantly better PFS and OS (log rank p < 0.05 for both). Our findings show that

genotypic, single-cell identification of pPCs in PC dyscrasias has relevant pathogenic and clinical implications.

INTRODUCTION

Multiple myeloma (MM) is a plasma cell (PC) neoplasm whose origin is in the germinal center of a secondary follicle[1,2]. Initiating somatic events at the genomic level are thought to be translocations of recurrent oncogenes to the immunoglobulin heavy chain (IGH) locus, or trisomies of several odd-numbered chromosomes[1]. Asymptomatic PC expansions can be categorized as monoclonal gammopathy of undetermined significance (MGUS) or smoldering multiple myeloma (SMM) based on the bone marrow (BM) monoclonal PC percentage[3–5]. Evolution from MGUS to SMM and MM is paralleled by the acquisition of secondary somatic genomic events, such as gene mutations, further translocations and copy-number abnormalities (CNAs)[6–8]. However, the serial study of MM samples evolved from SMM shows that some cases do not display genomic changes[9,10]. Here, transformation to an aggressive clone has likely already happened. However, it is possible that not all clinical progressions are explained by genomics alone: indeed, a disrupted tumor microenvironment (TME) plays a clear pathogenic role in MM development[11,12] by providing pro-survival and anti-apoptoticstimuli[13–16]. Furthermore, surveillance from immune TME cells has the potential to prevent evolution of asymptomatic stages of PC dyscrasias[17], and is disrupted along their progression[11,15,18,19,20]. Strategies to restore anti-MM immune function are a promising treatment approach in relapsed-refractory MM (RRMM) cases, where high-risk genomic lesions are enriched and response to conventional treatments is poor[20–22,23]. Indeed, in the era of novel immunotherapies, the quality of response depends not just on escape mechanisms by tumor cells, but also on effector cell function[24–28]. Immunoparesis, defined as reduced levels of one or more non-clonal immunoglobulin classes, is frequent in PC dyscrasias. Its prevalence increases from MGUS to SMM and MM and has prognostic value[29–31]. In MM, immunoparesis can explain the increased susceptibility to infection and is associated with an overall worse prognosis[31,32]. Clearly, immunoparesis can only be explained by disruption of polyclonal PCs. However, little is known about the functional properties of polyclonal PCs (pPCs) in various stages of PC dyscrasias.

Single cell RNA sequencing (scRNAseq) has the potential to dissect the clonal and polyclonal PC populations, and initial studies have found a different transcriptomic signature of the two populations[32–34]. However, our studies[35] and others [33,34] have shown that polyclonal PCs do not always clearly separate from clonal PCs in scRNAseq Uniform Manifold Approximation

and Projection (UMAP) plots, suggesting that a pure transcriptomic approach may be imperfect to accurately identify pPCs. Newer technologies allowing single-cell B-cell receptor (BCR) genotyping along with transcriptome sequencing of the same single-cell are better suited for this task. In this paper, we developed an algorithm to unambiguously identify polyclonal PCs at the single-cell genotypic level. This allowed us to study their functional properties in MGUS, SMM and MM stage as well as in comparison with normal PCs from healthy donors (HD), showing they have profoundly deranged functions impacting the TME, the production of polyclonal immunoglobulins, that ultimately correlate with disease progression and prognosis.

MATERIALS AND METHODS

A detailed description of all methods is presented in the supplemental Methods.

Sample selection

BM aspirates from of n= 46 patients affected by MGUS (n=7), SMM (n=16) and MM (n=23) were obtained at Fondazione IRCCS Ca' Granda Ospedale Maggiore Policlinico, Milan (Italy), according to IMWG criteria[5] as well as four sample from healthy donor (HD). Detailed clinical information for each case is provided in **Table S1.**

N = 3 HDs were collected from Erasmus MC Cancer Institute, Rotterdam, (Netherlands). N=14 (HDs) samples were obtained from publicly available databases[33,36] .

Sample processing

Mononuclear cells (MNCs) were used by Ficoll-Paque medium (Cytiva, Cat# 17144002) density gradient centrifugation and CD138+ BM cells were prepared using the EasySep™ CD138 Positive selection kit II (STEMCELL Technologies, Cat#17887A), after erythrocyte lysis (Cytognos, Cat# CYT-BL), following manufacturer's instructions.

Single-cell RNA 5' sequencing library construction and sequencing

The Chromium Next GEM Single Cell 5' v2 protocol (CG000330 Rev E), was applied and Single-cell 5' RNA-seq libraries were generated following standard manufacturer's protocols. BCR Amplification Kit (10X Genomics; PN-2000253) was used for V(D)J analysis. Generated libraries were sequenced on a NovaSeq6000 platform (Illumina sequencing system) using a 150bp Paired End protocol, targeting approximately 100,000 reads/cell and 15,000 reads/cell for 5' gene expression and V(D)J enriched libraries, respectively, according to manufacturer's recommendations.

CD138+ pre-processing single-cell RNA sequencing analysis

The gene expression (GEX) and V(D)J sc-RNA seq data were aligned and quantified using the Cell Ranger (v 7.1) pipeline (https://www.10xgenomics.com/) and Seurat pipeline (v 4.4.0,) was used to analyze expression matrices.

Polyclonal cell selection

To analyze genotypically identified pPCs, a multistep process was applied, defining the dominant clonotype and the nucleotide sequence of the CDR3 of any non-clonal clonotype, followed by Immcantation pipeline[37,38] and inferCNV analysis (https://github.com/broadinstitute/inferCNV).

Plasma cells single-cell RNA sequencing analysis

Sc-RNA seq analysis was performed by Seurat pipeline, using the RPCA method for integration. The integrated Seurat object was scaled, and the batch effect was corrected by Harmony[39] (v.1.2.0), before the functional enrichment analysis . In order to avoid cell clustering confounding factors, immunoglobulin related genes (genes located in IGH, IGL or IGK loci), were removed for downstream analyses.[11,33,35,40]

Single-cell copy number variation analysis

Copy number alterations (CNAs) were inferred from single cell gene expression data using inferCNV R package[41] (v 1.16.0, https://github.com/broadinstitute/inferCNV).

Single-cell HD signature definition and scoring

HD gene signature was defined by a differential gene expression analysis ("wilcoxauc" R function) between HDs and MGUS, SMM and MM, and only genes significantly upregualted in HDs (Benjamini—Hochberg adjusted p.value < 0.05, logFoldchange > 0.1) were retained. Then, intersection of deregulated genes within each contrast using the "distinct" mode was calculated (ComplexHeatmap (v 2.18.0)).

Finally, the HD gene expression signature was inferred in MMRF bulk RNA-sequencing dataset (IA17 release, https://research.themmrf.org). Survival analysis was performed using survival (v 3.5-8) and survminer (v 0.4.9) packages.

CD138- pre-processing single-cell RNA sequencing analysis

GEX and V(D)J scRNA-seq data of matched n=31 CD138- samples (n=23 fresh and N=8 frozen) were pre-processed using the Cell Ranger pipeline (v7.1).

Cell-cell communication and interaction analysis

Interaction analysis was performed using the MultiNicheNet package (v 1.0.3)[42] implemented in R (https://github.com/saeyslab/multinichenetr). The analysis includes 31 matched samples, and it was performed integrating CD138+ cells and CD138- cells for the TME. Comparisons were conducted between patients with and without immunoparesis[31].

RESULTS

Landscape of polyclonal plasma cells across stages of PC dyscrasias

We analyzed CD138-purified samples from 7 MGUS, 16 SMM and 23 MM patients. CD138+ samples from HD were sourced locally (n = *4*), from collaborators (n = *3*), and from publicly available databases (*n* = 14)[33,36]. For patients with PC dyscrasias (**Table S1)**, we developed a workflow (**Figure 1A**) to leverage single-cell data to genotypically identify clonal *vs* polyclonal PCs. The polyclonal nature of the latter group was confirmed by the lack of identity and hierarchical relationship of the heavy and light chain BCR sequence with the BCR sequence of clonal PCs of the same patient (**Table S2**). PCs sharing the same light chain, or substantial identity with the clonal sequence were excluded from analysis (**Materials and Methods, Table S2**). Copy-number abnormalities (CNAs) analysis through InferCNV[41] confirmed that pPCs of each individual sample did not share any of the CNAs observed in their cPCs counterparts, both in supervised and unsupervised analysis (**Figure S1-S4, S5**). After filtering cells, a total of n= *234,789* PCs (n=*54,419* from HDs, n= *15,882* from MGUS, n= *55,409* from SMM and n= *109,079* from MM) (**Figure 1B**) were used for further analysis. Using this approach, n= *170,357* cells (72,55%) were genotyped as clonal (cPCs) and n= *64,432* (27,44%) as polyclonal (pPCs). Overall, the frequency of pPCs was higher for MGUS and decreased in SMM and MM samples. In MGUS, the mean percentage of pPCs was 23.66% (range 6.34%-46.77%), whereas in SMM it dropped to 10.10% (1.14%-52.69%), and in MM to 3.23% (0.25%-23.65%) (p=0.00012, chi-squared test) (**Table S3)**. The absolute number of pPCs followed a similar trend, with n= *3,103* (19.53%) in MGUS, n= *3,291* (5.93%) in SMM, and n= *3,619* (3.31%) in MM (**Figure 1B-C)**.

We first analyzed cells in bulk, i.e. merging the transcriptome of each single cell in a single "polyclonal" vs "clonal" plasma cell sample for all MGUS, SMM and MM patients. pPCs were quite similar to cPCs in MGUS, with no differentially expressed genes. In turn, differentially expressed genes were found in SMM and MM as expected (**Figure S6**). However, the strength of scRNAseq is to evaluate the contrasts between thousands of cells per sample without losing each individual signal, therefore retaining the heterogeneity of each sample and each cell within the sample. Performing this analysis, in the UMAP sample space, pPCs from different individuals tended to cluster together. However, there also was a considerable

admixture of pPCs and cPCs in the sample space of each patient (**Figure 1D, Figures S7, S8, S9A**), indicating that transcriptomics alone may fail to accurately dissect every pPC from cPCs. The UMAP distribution of cells by disease stage showed how PCs from MGUS, SMM and MM were progressively more distant from PC from HD, as expected (**Figure 1E, S9B**). When stratified by FISH, PC tended to cluster by cytogenetic group rather than by symptomatic stage (**Figure S10**). We next looked at canonical PC marker genes. Our analysis confirmed previous observations, such as the frequent loss of *CD27* [33,43,44] in cPCs, and their uniform expression of *CD38*, *CD138* and *BCMA (TNFRSF17)* (**Figure 1F**). As expected, oncogenes such as *NSD2* and *CCND1/2,* and *MAF* were only expressed in cPCs. Interestingly, we found *GPRC5D* expression to be on average lower in pPCs than in cPCs from the same patients, differently from BCMA. (**Figure S11**). This might explain the lower risk of infections of anti-GPRC5D T-cell redirecting immunotherapies as compared anti-BCMA treatments[25]. Of note, pPCs frequently expressed markers usually attributed to cPCs such as *IGTB7*, *CCND3*, and this was true for both pPCs from patients and PCs from HDs (**Figure 1F**).

Polyclonal PCs from patients show deregulated expression profiles and an inflammatory phenotype

We next restricted our analysis to the phenotype of n= *64,432* pPCs to determine their transcriptomic heterogeneity. After filtering cells using standard quality controls (**Figure S12A-C**), pPCs were re-plotted along with PCs from HDs: here, we observed a slight divergence of cells from patients and HDs, but overall there was a considerable overlap of cells from all disease stages (**Figure 2A**). After creating UMAP plots by clusters and by patients (**Figure S13A-B**), we next asked what genes are differentially expressed in the different clinical categories. Analysis of differentially expressed genes showed that pPCs from patients had a similar pattern, different from HDs (**Figure 2B**). The latter group showed overexpression of genes such as *DUSP1*, *BTG1*, *FKBP2* and *NFAKB1A*, mainly involved in controlling MAPK (mitogen activated kinase-like protein) signaling, protein folding and protection against oxidative stress. Conversely, in pPCs from patients we found upregulation of genes usually associated with inflammation and/or stress conditions (*i.e*. *IRF1, ISG15, IFITM1*), such as the autophagy receptor *SQSTM1*, and the *VIM* gene, often upregulated during epithelial to mesenchymal transition (**Figure 2B)**. Canonical PC marker genes were

not different between pPCs in patients and HDs. Other genes were instead exclusively expressed in pPCS from patients, such as *CTSB*, *CTSD*, *OPTN* involved in autophagy. Even more interestingly, we found that only PCs from SMM and MM upregulated the surface integrin *ICAM1*, implying that interaction with the TME changes for pPCs in more advanced stages (**Figure 2C**). We performed a differential expression (DE) analysis to look at pathway analyses in all possible 1:1 contrast combinations (Wilcoxon rank sum test, with *padjust* Benjamini-Hochberg correction): there was an upregulation of inflammatory pathways (hallmark TNF α and IFN α response, hallmark oxidative phosphorylation) in pPCs from patients as compared to HDs, as well as comparing pPCs across disease stages to each other, with the most clear-cut differences between MGUS and SMM/MM (**Figure 3A, Figure S14 A-C)**. Statistics are reported in **Table S4**. In summary, we showed a *climax* of increasing inflammatory status in pPCs from HD to MM (**Figure 3B-D, Figure S14 A-C)**.

Single-cell transcriptomic correlates of immunoparesis

Production of polyclonal immunoglobulins in patients with plasma cell dyscrasias is impaired to variable extents. Particularly, reduction in the production of uninvolved immunoglobulins is seen as a risk factor for progression in asymptomatic conditions[31,45], and as a risk factor for survival and infections in MM, where it also predicts lower response to vaccination[46,47,48,49]. Our unique dataset allowed us to specifically characterize the transcriptional profiles of pPCs in patients with and without immunoparesis, defined as the decrease of one or more of the uninvolved immunoglobulin classes[31]. Having shown the presence of strongly enriched inflammatory pathways in pathological pPCs, we next sought to define their expression profile in immunoparesis-positive patients.

Of n= 46 patients (n=*10,013* pPCs) (**Figure 4A)**, 38 showed immunoparesis. We first observed that pPCs frequency tended to decline in patients showing immunoparesis (**Figure S15A-D**), likely explaining at least in part the decreased production of immunoglobulins. We next analyzed their gene expression profile. The immunoparesis-negative patients showed the expression of genes related to NF-KB (*i.e*. *BIRC3*), cell adhesion (*i.e. CXCR4, SDC1* and *PECAM1*), autophagy (*i.e. FOS, CST3*) and anti-apoptotic (*i.e. DYNLL*1) pathways. As compared to pPCs in patients without immunoparesis, pPCs in patients with immunoparesis showed upregulation of genes related to the interferon pathway (*i.e*. *IRF1, MX1* and *ISG15*), Unfolded Protein Response (UPR) (*ERN1*), cell proliferation and apoptosis (*i.e. H3F3B* and *NOP53*),

implying a more deregulated transcriptome (**Figure 4B)**. Then, to explore the functional consequences of gene expression deregulation we performed DE analysis comparing the immunoparesis status within the subset of symptomatic patients (n=23). Here, in presence of immunoparesis pPCs were functionally enriched for interferon related pathways (hallmark IFN γ) and oxidative phosphorylation **(Figure 4C-D).** Statistics are reported in **Table S5.** Taken together, our results reveal consistent changes in expression profiles of pPCs in immunoparesis- positive patients and correlate the presence of a pro-inflammatory phenotype with decreased immunoglobulin production.

The interactome landscape of immunoparesis in polyclonal PCs

Since progression and persistence of MM are influenced by the BM TME, and functional properties of both cPCs and pPCs are clearly dependent on interactions with the TME, we next investigated the cell-cell interactions between PCs repertoire and TME in the BM. To gain a first insight into the composition of the TME, we performed scRNA-seq of n=31 paired CD138+ and CD138- cell fractions within our cohort. In total, we integrated *n= 171,928* cells into a single dataset and used the MultiNicheNet pipeline[42], a tool that infers cell-cell interactions based on ligand-receptor expression and on the pathway activation downstream of the ligand in different cell types. To untangle the complexity of the TME**,** cPC n= *102,194*, pPC n= *7,447*, and TME cells n=*62,287* were analyzed (**Table S6**). The TME and the PCs' compartment mapped separately in UMAP plots (**Figure 5A**). Here, we found, n= *148,006* cells of n=23 (*n=89,037* cPCs, n=*3923* pPCs, n=*55,046* TME) characterized by immunoparesis and n= *23,922* cells from n=8 immunoparesis-negative samples (n= *13,157* cPCs, n= *3,524* pPCs, n= *7,241 TME*) (**Figure 5B**). Splitting the TME data by cell type, n=*32,966* T cells, n=*3,472* B cells, n=*15,261* myeloid cells, n= *6,589* NK cells, n=*1,019* dendritic cells and n=*2,980* HSCs were analyzed and no significant differences were observed in the relative composition of the TME populations between immunoparesis-positive and immunoparesis-negative patients **(Figure 5B, Table S6, Figure S16)** with the known exception of a significant depletion of pPCs in immunoparesis-positive patients (*padjust = 0.004*) (**Figure S16**).

To understand disruption of inter-cellular relationships in this scenario, we first analyzed the immunoparesis-negative setting. Comparing top-ranked ligand-receptor interactions and analyzing the downstream targets, pPCs were predicted to be able to send signals to specific cell compartments such as pPCs, CD8-effector, CD8 memory and progenitor RBC cells **(Figure**

5C, Figure S17A-B). Mining PCs as senders, of relevance were the *CD38: PECAM1* (CD31) cell interaction -with a role in regulation of cell migration-, and a broad spectrum of interactions mediating cell adhesion involving *ICAM2, ICAM3* and *ITGB2* (T lymphocytes), already described in promoting cell survival processes.[50–54] Furthermore, cPCs and pPCs displayed the ability to receive signals from myeloid (DCs, HSCs, monocytes, pDC and Mk progenitor cells) and lymphoid (CD8 effectory, CD8 memory, NK, progenitor B and MAIT cells) compartments.

In this scenario, immune and inflammatory responses were driven by the specific interaction of THBS-1 (in monocytes and Mk progenitor cells) with *SDC1* (in pPCs) and *ITGA6* (in pPCs), as well as by the signaling of *HMGB-1* (in HSCs, NK, pDCs, MAIT, CD8 cells, progenitor B cells and monocytes) :*SDC1* (in pPCS). In addition, we found the *CCL5:SDC1* ligand-receptor interactions between T cells and cPCs/pPCs, known to be involved in tumor cell migration[55]. Looking at the downstream deregulated gene targets, derived by ligand-target correlation, genes implicated in the autophagy axis and in ER stress (*BNIP3, MT1X, MT2A*)[56,57] were upregulated as well as B cell survival pathways regulators (*i.e. CD74* and *ITGA6*)[58] (**Figure S18A-B**). These findings highlight an active involvement of pPCs in the pro/inflammatory TME in immunoparesis-negative cell landscape. However, pPCs in this setting maintain their functional role through autophagy, ER stress regulation and B cell survival pathway activation.

Conversely, cPCs became the main contributor of TME interactions in the immunoparesis-positive cell landscape, where a significant depletion of pPCs:TME interactions was observed (**Figure 5D, Figure S19A,B)**. These differences were not simply determined by a depletion of pPCs since the differential expression analyses are normalized for cell count.

In detail, cPCs and pPCs were characterized by the inflammatory signaling mediated by the *IFITM1:CD81* interaction (pPCs: pPCs, pPCs:CD8 effector/memory cells, Treg:pPCs), that is involved in IFN-gamma response pathway[59,60]. Of note, in this scenario where the interactions between myeloid compartment and pPCs were significantly depleted, DCs and pDCs were found to sustain pPCs survival through *BAFF-BCMA* axis[61–63].

Furthermore, the axis *TGFB2:TGFBR1/TGFBR2/ TGFBR3* mediated interactions between cPCs and CD8 T cells together with *TGFB1:ITGB1* (MAIT and NK with pPCs), suggesting a role of PCs in the immunosuppression of T-cell compartment. Of note, the γ-chain cytokine *IL-15* was shown to signal from pPCs in an autocrine manner to pPCs and in a paracrine manner to

cPCs by binding the common cytokine receptor γ chain (γ_c or *CD132*; encoded by the *IL2RG* gene) in the immunoparesis-negative setting. Conversely, in immunoparesis-positive patients, this cytokine signals from cPCs to cPCs and pPCs through the *IL15RA* receptor[64–67]. Only in this latter setting, the downstream signalling involves activation of pro-inflammatory pathways. Furthermore, downstream target genes related to inflammation and interferon pathways were upregulated (i.e. *IFI16, IFIT3, PLSCR1*)[68] as well as negative regulators of NF-kB pathway such as *TNFSF10*. Conversely, in this setting genes related to autophagy and B cell maintenance resulted downregulated (i.e. *CSTH, BNIP3, MTX1, MT2A*)[33,56] (**Figure S20A,B)**. Altogether these data support the presence of a pro-inflammatory status in immunoparesis-positive patients, driven by aberrant cellular interactions not found in immunoparesis-negative patients, likely impacting pPCs survival and function.

Signature analysis allows prediction of survival in independent datasets

The presence of residual normal PCs has been correlated with prognosis in MM patients[32,33]. Our data show that even pPCs in patients can be profoundly dysregulated and different from normal PCs in HDs. Our unique dataset therefore allowed us to generate a "healthy PC" (hPC) signature through the union of the differentially expressed genes in the three contrasts of PCs from HD with pPCs from MGUS, SMM, and MM patients respectively. Importantly, our hPC signature corrects for the dysregulated expression of pPCs in patients and incorporates a total of *n=158* genes (**Figure 6A**, **Table S7**) representing genes truly expressed in hPCs only. Applying the hPC signature in our cohort, a gradient could be observed whereby the signature was enriched in HD, and progressively less represented in pPCs from MGUS, SMM and MMs cases (**Figure 6B**).

Finally, we determined if enrichment for the hPC signature could have a clinical impact within a NDMM population. We hypothesized that in bulk RNAseq generated from CD138-selected cells part of the signal could be generated by pPCs, and our single-cell derived signature could identify the relevant genes even if expressed in a minority of cells. We therefore interrogated the RNAseq data of CoMMpass[69] and ranked patients based on the fractional representation of the hPCs signature. A simple categorical distinction based on the enrichment of the hPCs signature above and below the median clearly separated patients based on their survival. Specifically, the median progression-free survival (PFS) was 3.36 years [95% confidence interval, 2.75-4.23 years] in patients above the median and 2.47 years

[95% confidence interval, 1.99-3.18 years] in patients below the median (*p.value* = 0.015, log-rank test, **Figure 6C**). Median overall survival (OS) was not reached in patients above the median and was 5.87 years [5.36- not reached years] in patients below the median (*p.value*= 0.048, log-rank test, **Figure 6D**). Based on these results we assume that the hPCs signature might represent a surrogate of residual functional "polyclonality" within the BM and has prognostic value**.**

DISCUSSION

The TME architecture has long been implicated in initiation and evolution of PC dyscrasias. pPCs are an obvious component of the TME but have been understudied despite a clear biological and clinical relevance. Part of this depends on technical issues. For example, pPCs cannot be separated from cPCs based on isolation with magnetic beads while doing so with flow-sorting is complicated and not easily performed by most laboratories. In this scenario, we applied a comprehensive approach including sc-RNA sequencing coupled with BCR genotyping to unambiguously identify and study pPCs.

Using this advanced approach, we provide evidence that pPCs would not necessarily be identified with accuracy based on transcriptomics alone. Indeed, after removing immunoglobulin genes, i.e. highly expressed cell-specific genes accounting for a big part of the transcriptomic diversity between PCs, pPCs did not necessarily segregate away from cPCs from the same patient in the UMAP space, suggesting they might be themselves phenotypically aberrant. This is different from previous studies[33], and can be explained at least in part by the innovative methodology we employed.

pPCs from patients showed the expected differential expression of canonical marker genes as compared to cPCs. However, we also convincingly show that GPRC5D expression is natively lower in pPCs than in cPCs, a finding which may suggest that anti-GPRC5D bi-specific antibodies may relatively spare pPCs and explain the lower prevalence of infections in such patients contrary to anti-BCMA antibodies[70].

Moreover, our data reveal a profoundly dysregulated transcriptomic landscape of pPCs from patients affected by asymptomatic or symptomatic PC dyscrasias when compared to BM PCs derived from HDs sourced with a broad age range. In this setting, pPCs showed upregulation of *IFITM1, SQTM1*, *CTSB*, *CTSD*, *OPTN*[59,60] markers as well as *ICAM1*[71–75], implying an upregulation of inflammation, autophagy and interferon pathways, with a climax from asymptomatic to symptomatic patients . Of note, the primary purpose of autophagy is to sustain the cellular homeostasis in extreme conditions[76], such as the ones promoted by oxidative and proteotoxic stress due to an intense production and secretion of immunoglobulins[76–78]. Therefore, autophagy is fundamental for long-lived PCs to optimize the protein metabolism and the cell viability[77–80] and we believe that this pathway is exaggerated in the setting of residual pPCs with the BM of patients with PC dyscrasias. Our

findings also have translational implications. Patients showing immunoparesis had the lowest number of residual pPCs, and these cells were in turn also functionally aberrant. Indeed, pPCs derived from immunoparesis-positive patients showed upregulation of *IRF1, MX1* and *ISG15, ERN1, H3F3B* and *NOP53* genes suggesting activation of IFNα and IFNγ pathways, UPR and cell proliferation/apoptosis signaling in the suppression of uninvolved immunoglobulins. We further extended this analysis by looking at intercellular interactions between PCs and the TME within each patient, providing evidence of an inflamed TME in immunoparesis-positive patients. In this scenario, we observed a significant decrease in the number of interactions of pPCs with other immune cells in the TME. Furthermore, pPCs were characterized by a pro-inflammatory transcriptome, characterized by the interaction between IFITM1 and CD81 and the activation of the TGFB2:TGFBR1/TGFBR2/TGFBR3 axis that we see in our patients were indeed shown to be mainly driven by IFN pathways and may affect pPCs survival and function, including production of IgM and IgG[81]. Altogether, our findings shed new light on mechanisms of deregulated pPCs homeostasis leading to immunoparesis in patients affected by PC dyscrasias. Furthermore, based on previous studies[82–84] we speculate that in these conditions the immune microenvironment could be less competent in antigen-presenting activity as well as in immunosurveillance, further adding to the complex interrelationships between antibody production, immunity and tumor progression. Whether this was solely related to the burden of clonal PCs producing more inflammation in the TME thus impacting the number and function of residual pPCs, or other factors influence these findings is something that will need to be further investigated.

Our data do not necessarily identify the primary cause of an inflamed TME. cPCs may be responsible through perturbed interaction with pPCs and other cells in the TME. However, it can also be argued that a pro-inflammatory TME can itself have a primary driver role, deranging the normal BM PC transcriptional program and thus promoting the growth of pre-existing cPCs -harboring initiating genomic lesions- whose proliferative potential was not expressed until then. The notion that cPCs can progress to an overt MM without acquiring new genomic events and thus potentially based on microenvironmental stimuli, is indeed quite substantial[85,80] and our data shed some light for the first time on the type of selection applied from the TME on BM polyclonal PCs.

Intriguingly, we also identified a specific “healthy” PC signature by comparing PCs from HD with pPCs of patients rather than to total CD138+ cells, which resulted decreased across

disease-stages and anti-correlated with the immunoparesis signature. Notably, this signature can be applied to bulk RNAseq. In the CoMMpass dataset, patients with an HD signature enrichment over the median showed a better PFS and OS. Given the PC-specific nature of the signature, this is not a result of less pure sampling. Rather, these findings emphasize the role of residual "functional polyclonality" within BM PCs, suggesting that the maintenance of a normal polyclonal population -and/or less transcriptionally disrupted cPCs- impacts on patient's survival[82,86].

In conclusion, our study employs a new methodology of analysis to gain deep insights into transcriptional landscape of pPCs in PCs dyscrasias, suggesting they are impacted by TME disruption just as other immune cells. Their dysfunction therefore can be used as a proxy for TME disruption promoted by MM and has biological and clinical consequences whose understanding may impact research and treatment of MM.

ACKNOWLEDGMENTS

This work was supported by the European Research Council under the European Union's Horizon 2020 research and innovation program (grant agreement No. 817997), by International Myeloma Society (IMS) and Paula and Rodger Riney Foundation Translational Research Grant Application-2023 and by Associazione Italiana Ricerca sul Cancro (IG25739). AIRC IG 24365 to AN. M.C.D.V. was funded by Umberto Veronesi Foundation and by Pfizer Global Medical Grants (grant tracking No. 75340503). "Fondo per il Programma Nazionale di Ricerca e Progetti di Rilevante Interesse Nazionale—PRIN" (project n.2022ZKKWLW to AGS). This study was supported in part by Italian Ministry of Health—Current research IRCCS.

AUTHOR CONTRIBUTIONS

N.B., **M.C.D.V. F.L.,** conceived the project; **N.B., M.C.D.V., F.L.,** designed the experiments; **N.B., M.C.D.V., C.D.M, L.P.,** enrolled and followed up patients and acquired data; **M.C.D.V., F.L., A.M., A.M.,** performed single cell experiments; **A.M.** verified the raw data before analyses and performed pre-processing bioinformatic analysis; **M.C.D.V., F.L., A.M.,** performed the bioinformatic analysis and interpreted data; **M.L., S.P., S.F., E.C., S.L., M.S., N. L., G. C., A.G.S., V.D.S., G.M.P., L.M., R.G., A.N., F.T., K.F., T.C., F.P.,** contributed with scientific discussions; **A.C., M.T.,** performed the flow cytometry experiments; **N.B., F.L., A.M., M.C.D.V.,** wrote the manuscript, which has been revised by all the authors.

Declaration of interests

N.B. received honoraria for Amgen, GSK, Janssen, Jazz, Pfizer, Takeda.

M.C.D.V. served as Advisory Board for Takeda, Menarini, Amgen, Pfizer, Johnson & Johnson, and on Speakers Bureau for Johnson & Johnson, Sanofi and GSK. F.P. received honoraria during the last two years for lectures from Novartis, Bristol-Myers Squibb, Abbvie, GSK, Janssen, AOP Orphan and for advisory boards from Novartis, Bristol-Myers Squibb/ Celgene, GSK, Abbvie, AOP Orphan, Janssen, Karyiopharma, Kyowa Kirin and MEI, Sumitomo, Kartos.

The remaining Authors declare no competing financial interest. AGS has received speaker honoraria from Sanofi, Amgen, and AstraZeneca. He has also participated in advisory boards for Pfizer and Menarini and received travel support for educational purposes from Janssen-Cilag.

References

1. Morgan, G.J., Walker, B.A., and Davies, F.E. (2012). The genetic architecture of multiple myeloma. Nat Rev Cancer *12*, 335–348. https://doi.org/10.1038/nrc3257.
2. Da Via, M.C., Zicchedda, B., Maeda, A., Bagnoli, F., Perrone, G., and Bolli, N. (2020). A Journey Through Myeloma Evolution: From the Normal Plasma Cell to Disease Complexity. Hemasphere *4*, e502. https://doi.org/10.1097/HS9.0000000000000502.
3. Kyle, R.A., Larson, D.R., Therneau, T.M., Dispenzieri, A., Kumar, S., Cerhan, J.R., and Rajkumar, S.V. (2018). Long-Term Follow-up of Monoclonal Gammopathy of Undetermined Significance. N Engl J Med *378*, 241–249. https://doi.org/10.1056/NEJMoa1709974.
4. Kyle, R.A., Remstein, E.D., Therneau, T.M., Dispenzieri, A., Kurtin, P.J., Hodnefield, J.M., Larson, D.R., Plevak, M.F., Jelinek, D.F., Fonseca, R., et al. (2007). Clinical Course and Prognosis of Smoldering (Asymptomatic) Multiple Myeloma. New England Journal of Medicine *356*, 2582–2590. https://doi.org/10.1056/NEJMoa070389.
5. Rajkumar, S.V., Dimopoulos, M.A., Palumbo, A., Blade, J., Merlini, G., Mateos, M.-V., Kumar, S., Hillengass, J., Kastritis, E., Richardson, P., et al. (2014). International Myeloma Working Group updated criteria for the diagnosis of multiple myeloma. The Lancet Oncology *15*, e538–e548. https://doi.org/10.1016/S1470-2045(14)70442-5.
6. Bolli, N., Avet-Loiseau, H., Wedge, D.C., Van Loo, P., Alexandrov, L.B., Martincorena, I., Dawson, K.J., Iorio, F., Nik-Zainal, S., Bignell, G.R., et al. (2014). Heterogeneity of genomic evolution and mutational profiles in multiple myeloma. Nat Commun *5*, 2997. https://doi.org/10.1038/ncomms3997.
7. Bolli, N., Biancon, G., Moarii, M., Gimondi, S., Li, Y., de Philippis, C., Maura, F., Sathiaseelan, V., Tai, Y.-T., Mudie, L., et al. (2018). Analysis of the genomic landscape of multiple myeloma highlights novel prognostic markers and disease subgroups. Leukemia *32*, 2604–2616. https://doi.org/10.1038/s41375-018-0037-9.
8. Maura, F., Bolli, N., Angelopoulos, N., Dawson, K.J., Leongamornlert, D., Martincorena, I., Mitchell, T.J., Fullam, A., Gonzalez, S., Szalat, R., et al. (2019). Genomic landscape and chronological reconstruction of driver events in multiple myeloma. Nat Commun *10*, 3835. https://doi.org/10.1038/s41467-019-11680-1.
9. Bolli, N., Maura, F., Minvielle, S., Gloznik, D., Szalat, R., Fullam, A., Martincorena, I., Dawson, K.J., Samur, M.K., Zamora, J., et al. (2018). Genomic patterns of progression in smoldering multiple myeloma. Nat Commun *9*, 3363. https://doi.org/10.1038/s41467-018-05058-y.
10. Oben, B., Froyen, G., Maclachlan, K.H., Leongamornlert, D., Abascal, F., Zheng-Lin, B., Yellapantula, V., Derkach, A., Geerdens, E., Diamond, B.T., et al. (2021). Whole-genome sequencing reveals progressive versus stable myeloma precursor conditions as two distinct entities. Nat Commun *12*, 1861. https://doi.org/10.1038/s41467-021-22140-0.

11. Botta, C., Perez, C., Larrayoz, M., Puig, N., Cedena, M.-T., Termini, R., Goicoechea, I., Rodriguez, S., Zabaleta, A., Lopez, A., et al. (2023). Large T cell clones expressing immune checkpoints increase during multiple myeloma evolution and predict treatment resistance. Nat Commun *14*, 5825. https://doi.org/10.1038/s41467-023-41562-6.
12. Bianchi, G., and Munshi, N.C. (2015). Pathogenesis beyond the cancer clone(s) in multiple myeloma. Blood *125*, 3049–3058. https://doi.org/10.1182/blood-2014-11-568881.
13. Hideshima, T., Mitsiades, C., Tonon, G., Richardson, P.G., and Anderson, K.C. (2007). Understanding multiple myeloma pathogenesis in the bone marrow to identify new therapeutic targets. Nat Rev Cancer *7*, 585–598. https://doi.org/10.1038/nrc2189.
14. de Jong, M.M.E., Fokkema, C., Papazian, N., Czeti, Á., Appelman, M.K., Vermeulen, M., van Heusden, T., Hoogenboezem, R.M., van Beek, G., Tahri, S., et al. (2024). An IL-1β-driven neutrophil-stromal cell axis fosters a BAFF-rich protumor microenvironment in individuals with multiple myeloma. Nat Immunol *25*, 820–833. https://doi.org/10.1038/s41590-024-01808-x.
15. de Jong, M.M.E., Kellermayer, Z., Papazian, N., Tahri, S., Hofste op Bruinink, D., Hoogenboezem, R., Sanders, M.A., van de Woestijne, P.C., Bos, P.K., Khandanpour, C., et al. (2021). The multiple myeloma microenvironment is defined by an inflammatory stromal cell landscape. Nat Immunol *22*, 769–780. https://doi.org/10.1038/s41590-021-00931-3.
16. Solimando, A.G., Da Vià, M.C., Leone, P., Borrelli, P., Croci, G.A., Tabares, P., Brandl, A., Di Lernia, G., Bianchi, F.P., Tafuri, S., et al. (2021). Halting the vicious cycle within the multiple myeloma ecosystem: blocking JAM-A on bone marrow endothelial cells restores angiogenic homeostasis and suppresses tumor progression. Haematologica *106*, 1943–1956. https://doi.org/10.3324/haematol.2019.239913.
17. Nakamura, K., Smyth, M.J., and Martinet, L. (2020). Cancer immunoediting and immune dysregulation in multiple myeloma. Blood *136*, 2731–2740. https://doi.org/10.1182/blood.2020006540.
18. Liu, R., Gao, Q., Foltz, S.M., Fowles, J.S., Yao, L., Wang, J.T., Cao, S., Sun, H., Wendl, M.C., Sethuraman, S., et al. (2021). Co-evolution of tumor and immune cells during progression of multiple myeloma. Nat Commun *12*, 2559. https://doi.org/10.1038/s41467-021-22804-x.
19. Pilcher, W.C., Yao, L., Gonzalez-Kozlova, E., Pita-Juarez, Y., Karagkouni, D., Acharya, C., Michaud, M.E., Hamilton, M., Nanda, S., Song, Y., et al. (2024). A single-cell atlas characterizes dysregulation of the bone marrow immune microenvironment associated with outcomes in multiple myeloma. Preprint, https://doi.org/10.1101/2024.05.15.593193 https://doi.org/10.1101/2024.05.15.593193.
20. Gulla', A., and Anderson, K.C. (2020). Multiple myeloma: the (r)evolution of current therapy and a glance into the future. Haematologica *105*, 2358–2367. https://doi.org/10.3324/haematol.2020.247015.
21. Zicchedda, B., Biancon, G., Bagnoli, F., De Philippis, C., Maura, F., Rustad, E.H., Dugo, M., Devecchi, A., De Cecco, L., Sensi, M., et al. (2020). Integrative analysis of the genomic and transcriptomic landscape of double-refractory multiple myeloma. Blood Advances *4*, 830–844. https://doi.org/10.1182/bloodadvances.2019000779.
22. Gulla, A., Morelli, E., Samur, M.K., Botta, C., Hideshima, T., Bianchi, G., Fulciniti, M., Malvestiti, S., Prabhala, R.H., Talluri, S., et al. (2021). Bortezomib induces anti-multiple myeloma immune response mediated by cGAS/STING pathway activation. Blood Cancer Discov *2*, 468–483. https://doi.org/10.1158/2643-3230.BCD-21-0047.
23. Maura, F., Boyle, E.M., Coffey, D., Maclachlan, K., Gagler, D., Diamond, B., Ghamlouch, H., Blaney, P., Zicchedda, B., Cirrincione, A., et al. (2023). Genomic and immune signatures predict clinical outcome in newly diagnosed multiple myeloma treated with immunotherapy regimens. Nat Cancer *4*, 1660–1674. https://doi.org/10.1038/s43018-

023-00657-1.
24. Friedrich, M.J., Neri, P., Kehl, N., Michel, J., Steiger, S., Kilian, M., Leblay, N., Maity, R., Sankowski, R., Lee, H., et al. (2023). The pre-existing T cell landscape determines the response to bispecific T cell engagers in multiple myeloma patients. Cancer Cell *41*, 711-725.e6. https://doi.org/10.1016/j.ccell.2023.02.008.
25. Lee, H., Ahn, S., Maity, R., Leblay, N., Ziccheddu, B., Truger, M., Chojnacka, M., Cirrincione, A., Durante, M., Tilmont, R., et al. (2023). Mechanisms of antigen escape from BCMA- or GPRC5D-targeted immunotherapies in multiple myeloma. Nat Med *29*, 2295–2306. https://doi.org/10.1038/s41591-023-02491-5.
26. Poos, A.M., Prokoph, N., Przybilla, M.J., Mallm, J.-P., Steiger, S., Seufert, I., John, L., Tirier, S.M., Bauer, K., Baumann, A., et al. (2023). Resolving therapy resistance mechanisms in multiple myeloma by multiomics subclone analysis. Blood *142*, 1633–1646. https://doi.org/10.1182/blood.2023019758.
27. Da Vià, M.C., Dietrich, O., Truger, M., Arampatzi, P., Duell, J., Heidemeier, A., Zhou, X., Danhof, S., Kraus, S., Chatterjee, M., et al. (2021). Homozygous BCMA gene deletion in response to anti-BCMA CAR T cells in a patient with multiple myeloma. Nat Med *27*, 616–619. https://doi.org/10.1038/s41591-021-01245-5.
28. Samur, M.K., Fulciniti, M., Aktas Samur, A., Bazarbachi, A.H., Tai, Y.-T., Prabhala, R., Alonso, A., Sperling, A.S., Campbell, T., Petrocca, F., et al. (2021). Biallelic loss of BCMA as a resistance mechanism to CAR T cell therapy in a patient with multiple myeloma. Nat Commun *12*, 868. https://doi.org/10.1038/s41467-021-21177-5.
29. Landgren, O., Hofmann, J.N., McShane, C.M., Santo, L., Hultcrantz, M., Korde, N., Mailankody, S., Kazandjian, D., Murata, K., Thoren, K., et al. (2019). Association of Immune Marker Changes With Progression of Monoclonal Gammopathy of Undetermined Significance to Multiple Myeloma. JAMA Oncol *5*, 1293. https://doi.org/10.1001/jamaoncol.2019.1568.
30. Cherry, B.M., Costello, R., Zingone, A., Burris, J., Korde, N., Manasanch, E., Kwok, M., Annunziata, C., Roschewski, M.J., Engels, E.A., et al. (2013). Immunoparesis and monoclonal gammopathy of undetermined significance are disassociated in advanced age. Am J Hematol *88*, 89–92. https://doi.org/10.1002/ajh.23355.
31. Pérez-Persona, E., Vidriales, M.-B., Mateo, G., García-Sanz, R., Mateos, M.-V., de Coca, A.G., Galende, J., Martín-Nuñez, G., Alonso, J.M., de Las Heras, N., et al. (2007). New criteria to identify risk of progression in monoclonal gammopathy of uncertain significance and smoldering multiple myeloma based on multiparameter flow cytometry analysis of bone marrow plasma cells. Blood *110*, 2586–2592. https://doi.org/10.1182/blood-2007-05-088443.
32. Ledergor, G., Weiner, A., Zada, M., Wang, S.-Y., Cohen, Y.C., Gatt, M.E., Snir, N., Magen, H., Koren-Michowitz, M., Herzog-Tzarfati, K., et al. (2018). Single cell dissection of plasma cell heterogeneity in symptomatic and asymptomatic myeloma. Nat Med *24*, 1867–1876. https://doi.org/10.1038/s41591-018-0269-2.
33. Boiarsky, R., Haradhvala, N.J., Alberge, J.-B., Sklavenitis-Pistofidis, R., Mouhieddine, T.H., Zavidij, O., Shih, M.-C., Firer, D., Miller, M., El-Khoury, H., et al. (2022). Single cell characterization of myeloma and its precursor conditions reveals transcriptional signatures of early tumorigenesis. Nat Commun *13*, 7040. https://doi.org/10.1038/s41467-022-33944-z.
34. Dang, M., Han, G., Lee, H.C., Patel, K.K., Becnel, M.R., Wang, R., Thomas, S.K., Hao, D., Chu, Y., Weber, D.M., et al. (2023). Single cell clonotypic and transcriptional evolution of multiple myeloma precursor disease. Cancer Cell *41*, 1032-1047.e4. https://doi.org/10.1016/j.ccell.2023.05.007.
35. Lazzaroni, F., Matera, A., Marella, A., Maeda, A., Castellano, G., Marchetti, A.,

Fabris, S., Pioggia, S., Silvestris, I., Ronchetti, D., et al. (2024). Inference of genomic lesions from single-cell RNAseq in myeloma improves functional intra- and inter-clonal analysis. Blood Advances, bloodadvances.2023012409. https://doi.org/10.1182/bloodadvances.2023012409.
36. Duan, M., Nguyen, D.C., Joyner, C.J., Saney, C.L., Tipton, C.M., Andrews, J., Lonial, S., Kim, C., Hentenaar, I., Kosters, A., et al. (2023). Understanding heterogeneity of human bone marrow plasma cell maturation and survival pathways by single-cell analyses. Cell Rep *42*, 112682. https://doi.org/10.1016/j.celrep.2023.112682.
37. Suo, C., Polanski, K., Dann, E., Lindeboom, R.G.H., Vilarrasa-Blasi, R., Vento-Tormo, R., Haniffa, M., Meyer, K.B., Dratva, L.M., Tuong, Z.K., et al. (2024). Dandelion uses the single-cell adaptive immune receptor repertoire to explore lymphocyte developmental origins. Nat Biotechnol *42*, 40–51. https://doi.org/10.1038/s41587-023-01734-7.
38. Gupta, N.T., Vander Heiden, J.A., Uduman, M., Gadala-Maria, D., Yaari, G., and Kleinstein, S.H. (2015). Change-O: a toolkit for analyzing large-scale B cell immunoglobulin repertoire sequencing data. Bioinformatics *31*, 3356–3358. https://doi.org/10.1093/bioinformatics/btv359.
39. Korsunsky, I., Millard, N., Fan, J., Slowikowski, K., Zhang, F., Wei, K., Baglaenko, Y., Brenner, M., Loh, P., and Raychaudhuri, S. (2019). Fast, sensitive and accurate integration of single-cell data with Harmony. Nat Methods *16*, 1289–1296. https://doi.org/10.1038/s41592-019-0619-0.
40. Verstegen, N.J., Pollastro, S., Unger, P.-P.A., Marsman, C., Elias, G., Jorritsma, T., Streutker, M., Bassler, K., Haendler, K., Rispens, T., et al. Single-cell analysis reveals dynamics of human B cell differentiation and identifies novel B and antibody-secreting cell intermediates. eLife *12*, e83578. https://doi.org/10.7554/eLife.83578.
41. Patel, A.P., Tirosh, I., Trombetta, J.J., Shalek, A.K., Gillespie, S.M., Wakimoto, H., Cahill, D.P., Nahed, B.V., Curry, W.T., Martuza, R.L., et al. (2014). Single-cell RNA-seq highlights intratumoral heterogeneity in primary glioblastoma. Science *344*, 1396–1401. https://doi.org/10.1126/science.1254257.
42. Browaeys, R., Gilis, J., Sang-Aram, C., De Bleser, P., Hoste, L., Tavernier, S., Lambrechts, D., Seurinck, R., and Saeys, Y. (2023). MultiNicheNet: a flexible framework for differential cell-cell communication analysis from multi-sample multi-condition single-cell transcriptomics data (Bioinformatics) https://doi.org/10.1101/2023.06.13.544751.
43. Jung, J., Choe, J., Li, L., and Choi, Y.S. (2000). Regulation of CD27 expression in the course of germinal center B cell differentiation: the pivotal role of IL-10. Eur J Immunol *30*, 2437–2443. https://doi.org/10.1002/1521-4141(2000)30:8<2437::AID-IMMU2437>3.0.CO;2-M.
44. Morgan, T.K., Zhao, S., Chang, K.L., Haddix, T.L., Domanay, E., Cornbleet, P.J., Arber, D.A., and Natkunam, Y. (2006). Low CD27 expression in plasma cell dyscrasias correlates with high-risk disease: an immunohistochemical analysis. Am J Clin Pathol *126*, 545–551. https://doi.org/10.1309/ELGMGX81C2UTP55R.
45. Sigurdardottir, E.E., Turesson, I., Lund, S.H., Lindqvist, E.K., Mailankody, S., Korde, N., Björkholm, M., Landgren, O., and Kristinsson, S.Y. (2015). The Role of Diagnosis and Clinical Follow-up of Monoclonal Gammopathy of Undetermined Significance on Survival in Multiple Myeloma. JAMA Oncol *1*, 168. https://doi.org/10.1001/jamaoncol.2015.23.
46. Pettine, L., Bortolotti, M., Fattizzo, B., Da Vià, M.C., Consonni, D., Pompa, A., Bolli, N., and Baldini, L. (2022). Response to SARS-CoV-2 vaccination and antibodies persistence in multiple myeloma patients. Hematol Oncol, 10.1002/hon.3051. https://doi.org/10.1002/hon.3051.
47. Kastritis, E., Zagouri, F., Symeonidis, A., Roussou, M., Sioni, A., Pouli, A.,

739 Delimpasi, S., Katodritou, E., Michalis, E., Michael, M., et al. (2014). Preserved levels of
740 uninvolved immunoglobulins are independently associated with favorable outcome in
741 patients with symptomatic multiple myeloma. Leukemia *28*, 2075–2079.
742 https://doi.org/10.1038/leu.2014.110.
743 48. Azeem, M.I., Nooka, A.K., Shanmugasundaram, U., Cheedarla, N., Potdar, S.,
744 Manalo, R.J., Moreno, A., Switchenko, J.M., Cheedarla, S., Doxie, D.B., et al. (2023).
745 Impaired SARS-CoV-2 Variant Neutralization and CD8+ T-cell Responses Following 3
746 Doses of mRNA Vaccines in Myeloma: Correlation with Breakthrough Infections. Blood
747 Cancer Discov *4*, 106–117. https://doi.org/10.1158/2643-3230.BCD-22-0173.
748 49. Konishi, Y., Sklavenitis-Pistofidis, R., Yue, H., Ferrari, F., Redd, R.A., Lightbody,
749 E.D., Russo, M., Perry, J., Horowitz, E., Justis, A.V., et al. (2022). Attenuated response to
750 SARS-CoV-2 vaccine in patients with asymptomatic precursor stages of multiple myeloma
751 and Waldenstrom macroglobulinemia. Cancer Cell *40*, 6–8.
752 https://doi.org/10.1016/j.ccell.2021.12.003.
753 50. Amici, S.A., Young, N.A., Narvaez-Miranda, J., Jablonski, K.A., Arcos, J., Rosas, L.,
754 Papenfuss, T.L., Torrelles, J.B., Jarjour, W.N., and Guerau-de-Arellano, M. (2018). CD38 Is
755 Robustly Induced in Human Macrophages and Monocytes in Inflammatory Conditions.
756 Front. Immunol. *9*. https://doi.org/10.3389/fimmu.2018.01593.
757 51. Andreata, F., Clément, M., Benson, R.A., Hadchouel, J., Procopio, E., Even, G.,
758 Vorbe, J., Benadda, S., Ollivier, V., Ho-Tin-Noe, B., et al. (2023). CD31 signaling promotes
759 the detachment at the uropod of extravasating neutrophils allowing their migration to sites of
760 inflammation. eLife *12*, e84752. https://doi.org/10.7554/eLife.84752.
761 52. Newman, P.J., and Newman, D.K. (2003). Signal Transduction Pathways Mediated
762 by PECAM-1. Arteriosclerosis, Thrombosis, and Vascular Biology *23*, 953–964.
763 https://doi.org/10.1161/01.ATV.0000071347.69358.D9.
764 53. Piedra-Quintero, Z.L., Wilson, Z., Nava, P., and Guerau-de-Arellano, M. (2020).
765 CD38: An Immunomodulatory Molecule in Inflammation and Autoimmunity. Front Immunol
766 *11*, 597959. https://doi.org/10.3389/fimmu.2020.597959.
767 54. Woodfin, A., Voisin, M.-B., and Nourshargh, S. (2007). PECAM-1: A Multi-
768 Functional Molecule in Inflammation and Vascular Biology. Arteriosclerosis, Thrombosis,
769 and Vascular Biology *27*, 2514–2523. https://doi.org/10.1161/ATVBAHA.107.151456.
770 55. Chen, K., Wang, Y., Hou, Y., Wang, Q., Long, D., Liu, X., Tian, X., and Yang, Y.
771 (2022). Single cell RNA-seq reveals the CCL5/SDC1 receptor-ligand interaction between T
772 cells and tumor cells in pancreatic cancer. Cancer Lett *545*, 215834.
773 https://doi.org/10.1016/j.canlet.2022.215834.
774 56. Le Guerroué, F., Eck, F., Jung, J., Starzetz, T., Mittelbronn, M., Kaulich, M., and
775 Behrends, C. (2017). Autophagosomal Content Profiling Reveals an LC3C-Dependent
776 Piecemeal Mitophagy Pathway. Mol Cell *68*, 786-796.e6.
777 https://doi.org/10.1016/j.molcel.2017.10.029.
778 57. Ullio, C., Brunk, U.T., Urani, C., Melchioretto, P., Bonelli, G., Baccino, F.M., and
779 Autelli, R. (2015). Autophagy of metallothioneins prevents TNF-induced oxidative stress and
780 toxicity in hepatoma cells. Autophagy *11*, 2184–2198.
781 https://doi.org/10.1080/15548627.2015.1106662.
782 58. Gore, Y., Starlets, D., Maharshak, N., Becker-Herman, S., Kaneyuki, U., Leng, L.,
783 Bucala, R., and Shachar, I. (2008). Macrophage migration inhibitory factor induces B cell
784 survival by activation of a CD74-CD44 receptor complex. J Biol Chem *283*, 2784–2792.
785 https://doi.org/10.1074/jbc.M703265200.
786 59. Narayana, S.K., Helbig, K.J., McCartney, E.M., Eyre, N.S., Bull, R.A., Eltahla, A.,
787 Lloyd, A.R., and Beard, M.R. (2015). The Interferon-induced Transmembrane Proteins,
788 IFITM1, IFITM2, and IFITM3 Inhibit Hepatitis C Virus Entry. J Biol Chem *290*, 25946–

25959. https://doi.org/10.1074/jbc.M115.657346.
60. Wilkins, C., Woodward, J., Lau, D.T.-Y., Barnes, A., Joyce, M., McFarlane, N., McKeating, J.A., Tyrrell, D.L., and Gale, M. (2013). IFITM1 is a tight junction protein that inhibits hepatitis C virus entry. Hepatology *57*, 461–469. https://doi.org/10.1002/hep.26066.
61. Novak, A.J., Darce, J.R., Arendt, B.K., Harder, B., Henderson, K., Kindsvogel, W., Gross, J.A., Greipp, P.R., and Jelinek, D.F. (2004). Expression of BCMA, TACI, and BAFF-R in multiple myeloma: a mechanism for growth and survival. Blood *103*, 689–694. https://doi.org/10.1182/blood-2003-06-2043.
62. Hengeveld, P.J., and Kersten, M.J. (2015). B-cell activating factor in the pathophysiology of multiple myeloma: a target for therapy? Blood Cancer Journal *5*, e282–e282. https://doi.org/10.1038/bcj.2015.3.
63. Shah, N., Chari, A., Scott, E., Mezzi, K., and Usmani, S.Z. (2020). B-cell maturation antigen (BCMA) in multiple myeloma: rationale for targeting and current therapeutic approaches. Leukemia *34*, 985–1005. https://doi.org/10.1038/s41375-020-0734-z.
64. Tinhofer, I., Marschitz, I., Henn, T., Egle, A., and Greil, R. (2000). Expression of functional interleukin-15 receptor and autocrine production of interleukin-15 as mechanisms of tumor propagation in multiple myeloma. Blood *95*, 610–618.
65. Sindaco, P., Pandey, H., Isabelle, C., Chakravarti, N., Brammer, J.E., Porcu, P., and Mishra, A. (2023). The role of interleukin-15 in the development and treatment of hematological malignancies. Front. Immunol. *14*. https://doi.org/10.3389/fimmu.2023.1141208.
66. Waldmann, T.A., Miljkovic, M.D., and Conlon, K.C. (2019). Interleukin-15 (dys)regulation of lymphoid homeostasis: Implications for therapy of autoimmunity and cancer. Journal of Experimental Medicine *217*, e20191062. https://doi.org/10.1084/jem.20191062.
67. Wang, Y., Zhang, Y., Yi, P., Dong, W., Nalin, A.P., Zhang, J., Zhu, Z., Chen, L., Benson, D.M., Mundy-Bosse, B.L., et al. (2019). The IL-15–AKT–XBP1s signaling pathway contributes to effector functions and survival in human NK cells. Nat Immunol *20*, 10–17. https://doi.org/10.1038/s41590-018-0265-1.
68. Dal Col, J., Lamberti, M.J., Nigro, A., Casolaro, V., Fratta, E., Steffan, A., and Montico, B. (2022). Phospholipid scramblase 1: a protein with multiple functions via multiple molecular interactors. Cell Commun Signal *20*, 78. https://doi.org/10.1186/s12964-022-00895-3.
69. Skerget, S., Penaherrera, D., Chari, A., Jagannath, S., Siegel, D.S., Vij, R., Orloff, G., Jakubowiak, A., Niesvizky, R., Liles, D., et al. (2024). Comprehensive molecular profiling of multiple myeloma identifies refined copy number and expression subtypes. Nat Genet *56*, 1878–1889. https://doi.org/10.1038/s41588-024-01853-0.
70. Rodríguez-Otero, P., Schinke, C.D., Chari, A., Lipe, B., Lavi, N., Rasche, L., Vishwamitra, D., Skerget, S., Verona, R., Ma, X., et al. (2023). Analysis of infections and parameters of humoral immunity in patients (pts) with relapsed/refractory multiple myeloma (RRMM) treated with talquetamab (tal) monotherapy in MonumenTAL-1. JCO *41*, 8020–8020. https://doi.org/10.1200/JCO.2023.41.16_suppl.8020.
71. Dragoni, S., Hudson, N., Kenny, B.-A., Burgoyne, T., McKenzie, J.A., Gill, Y., Blaber, R., Futter, C.E., Adamson, P., Greenwood, J., et al. (2017). Endothelial MAPKs Direct ICAM-1 Signaling to Divergent Inflammatory Functions. J Immunol *198*, 4074–4085. https://doi.org/10.4049/jimmunol.1600823.
72. Cavallaro, U., and Dejana, E. (2011). Adhesion molecule signalling: not always a sticky business. Nat Rev Mol Cell Biol *12*, 189–197. https://doi.org/10.1038/nrm3068.
73. Scott, D.W., Tolbert, C.E., Graham, D.M., Wittchen, E., Bear, J.E., and Burridge, K. (2015). N-glycosylation controls the function of junctional adhesion molecule-A. Mol Biol

Cell *26*, 3205–3214. https://doi.org/10.1091/mbc.E14-12-1604.
74. Gorina, R., Lyck, R., Vestweber, D., and Engelhardt, B. (2014). β2 integrin-mediated crawling on endothelial ICAM-1 and ICAM-2 is a prerequisite for transcellular neutrophil diapedesis across the inflamed blood-brain barrier. J Immunol *192*, 324–337. https://doi.org/10.4049/jimmunol.1300858.
75. Bui, T.M., Wiesolek, H.L., and Sumagin, R. (2020). ICAM-1: A master regulator of cellular responses in inflammation, injury resolution, and tumorigenesis. J Leukoc Biol *108*, 787–799. https://doi.org/10.1002/JLB.2MR0220-549R.
76. Oliva, L., and Cenci, S. (2014). Autophagy in plasma cell pathophysiology. Front Immunol *5*, 103. https://doi.org/10.3389/fimmu.2014.00103.
77. Pengo, N., and Cenci, S. (2013). The role of autophagy in plasma cell ontogenesis. Autophagy *9*, 942–944. https://doi.org/10.4161/auto.24399.
78. Pengo, N., Scolari, M., Oliva, L., Milan, E., Mainoldi, F., Raimondi, A., Fagioli, C., Merlini, A., Mariani, E., Pasqualetto, E., et al. (2013). Plasma cells require autophagy for sustainable immunoglobulin production. Nat Immunol *14*, 298–305. https://doi.org/10.1038/ni.2524.
79. Clarke, A.J., and Simon, A.K. (2019). Autophagy in the renewal, differentiation and homeostasis of immune cells. Nat Rev Immunol *19*, 170–183. https://doi.org/10.1038/s41577-018-0095-2.
80. Calcinotto, A., Brevi, A., Chesi, M., Ferrarese, R., Garcia Perez, L., Grioni, M., Kumar, S., Garbitt, V.M., Sharik, M.E., Henderson, K.J., et al. (2018). Microbiota-driven interleukin-17-producing cells and eosinophils synergize to accelerate multiple myeloma progression. Nat Commun *9*, 4832. https://doi.org/10.1038/s41467-018-07305-8.
81. Vazquez, M.I., Catalan-Dibene, J., and Zlotnik, A. (2015). B cells responses and cytokine production are regulated by their immune microenvironment. Cytokine *74*, 318–326. https://doi.org/10.1016/j.cyto.2015.02.007.
82. Sammut, S.-J., Galson, J.D., Minter, R., Sun, B., Chin, S.-F., De Mattos-Arruda, L., Finch, D.K., Schätzle, S., Dias, J., Rueda, O.M., et al. (2024). Predictability of B cell clonal persistence and immunosurveillance in breast cancer. Nat Immunol *25*, 916–924. https://doi.org/10.1038/s41590-024-01821-0.
83. Rashid, H.-O., Yadav, R.K., Kim, H.-R., and Chae, H.-J. (2015). ER stress: Autophagy induction, inhibition and selection. Autophagy *11*, 1956–1977. https://doi.org/10.1080/15548627.2015.1091141.
84. Xu, D., Jiang, W., Wu, L., Gaudet, R.G., Park, E.-S., Su, M., Cheppali, S.K., Cheemarla, N.R., Kumar, P., Uchil, P.D., et al. (2023). PLSCR1 is a cell-autonomous defence factor against SARS-CoV-2 infection. Nature *619*, 819–827. https://doi.org/10.1038/s41586-023-06322-y.
85. Das, R., Strowig, T., Verma, R., Koduru, S., Hafemann, A., Hopf, S., Kocoglu, M.H., Borsotti, C., Zhang, L., Branagan, A., et al. (2016). Microenvironment-dependent growth of pre-neoplastic and malignant plasma cells in humanized mice. Nat Med *22*, 1351–1357. https://doi.org/10.1038/nm.4202.
86. Yan, W., Shi, L., Xu, J., Li, L., Cui, J., Liu, Y., Zhou, J., Du, C., Yu, T., Zhang, S., et al. (2024). Clinical implications of residual normal plasma cells within bone marrow across various disease stages in multiple myeloma. Leukemia *38*, 2235–2245. https://doi.org/10.1038/s41375-024-02366-9.

884
885
886
887
888
889
890
891
892
893
894
895

FIGURE LEGENDS

Figure 1. Clonal and polyclonal cells identification in patients affected by plasma cell dyscrasias and healthy donors (HD).

(A) Schematic overview of cohort of samples and workflow of the study.

(B) Donut charts representing the distribution of clonal and polyclonal cells in plasma cell dyscrasias and healthy donors based on clinical stratification (HD: blue; MGUS: green; SMM: orange; MM: red). Numerical values are reported in the legend for category. Color legend of clonal and polyclonal cells as in (B).

(C) The proportions of clonal cells (red) and polyclonal cells (blue) in each sample.

(D) UMAP plot show all clonal (red) and polyclonal (blue) cells, with numerical values.

(E) UMAP representation of as per **(D),** colors indicate clinical stratification of samples. Numerical values and percentages are reported in the legend for each category.

(F) Violin plots showing distribution of expression of genes commonly upregulated in patients plasma cell dyscrasias, along with annotations of the clinical classification (top). Bar above violin plots summarize clinical type assignments. Color legend as in (**B** and **C**).

Figure 2. Polyclonal cell selection and marker genes expression by clinical stages.

(A) UMAP of scRNA-seq data of selected pPCs with colors indicating clinical clusters. Numerical values are reported in the legend for each category. Color legend of polyclonal cells as in Figure **1C.**

(B) Dot plot displaying the top twenty marker genes that distinguish each clinical state. The X-axis lists the clinical category, while the Y lists gene names. Circle size corresponds to the number of cells in the category expressing the gene of interest, while shade correlates with the level of expression.

(C) Violin plot showing expression pattern of selected PCs, adhesion/interaction and autophagy marker genes across all the clinical stages.

Figure 3. Transcriptional characterization of pPCs

(A) Cartoon depicting the deregulated expression profiles of pPCs, derived from 1:1 DE analyses by Wilcoxon test. Circle size corresponds to the number of cells in the category expressing the gene of interest, while shade correlates with the level of expression. Color code as in Figure **1C**.

(B-D) GSEA plots depicting the enrichment of signal pathways based on the hallmark gene set.

Figure 4. Transcriptomic landscape of immunoparesis

(A) Cartoon showing the pathological subset of patients (MGUS, SMM and MM), for downstream DE analyses. Color code as in Figure **1C**.

(B) Dot plot of top ten marker genes that distinguish immunoparesis-negative and immunoparesis-positive patients. The X-axis lists the clinical category, while the Y lists gene names. Circle size corresponds to the number of cells in the category expressing the gene of interest, while shade correlates with the level of expression. Light blue: immunoparesis-negative patients, yellow: immunoparesis-positive patients.

(C) DE analysis comparing the immunoparesis-negative and immunoparesis-positive patients within symptomatic subset of patients, using Wilcoxon rank sum test, with *padjust* pBenjamini-Hochberg correction. Color code as in Figure **4B**.

(D) Gene set enrichment analysis (GSEA) on the genes ranked by their contribution to hallmark oxidative phosphorylation, complement, interferon alpha and interferon gamma response

Figure 5. Predicted interactions of PCs with microenvironment

(A) UMAP representation of PCs integrated with TME, colors indicate TME cell types.

(B) UMAP plot of PCs integrated with TME colored according to immunoparesis. Color code as Figure **4C**.

(C) Circos plots illustrate ligand-receptor Interactions between pPCs (blue), cPCs (red) and TME, according to immunoparesis clinical status. Ribbon arrows indicate directionality of communication, from sender to receiver populations, while the arrow's color signifies the

specific sender cell type expressing the ligand. Upper panel: PCs were set as sender. Lower panel: PCs were set as receiver.

Figure 6. A «hPC» signature analysis allows prediction in independent datasets

(A) HD gene signature defined by a DE analysis between HDs and MGUS, SMM and MM. For each contrast genes significantly up-regualted in HDs (Benjamini—Hochberg adjusted p.value < 0.05, logFoldchange > 0.1) were retained. Venn diagram to show the intersection of deregualted genes within each comparison. Color code as Figure **1D**.

(B) Violin plot showing the inference of HD in the cohort of patients. Color code as Figure **1D.**

(C, D) Clinical impact of HD signature in CoMMpass RNAseq data. Progression-free survival (PFS) **(C)** and overall survival (OS) **(D)** Kaplan-Meier curves in the cohort of patients.

Figure 1

Fig.1

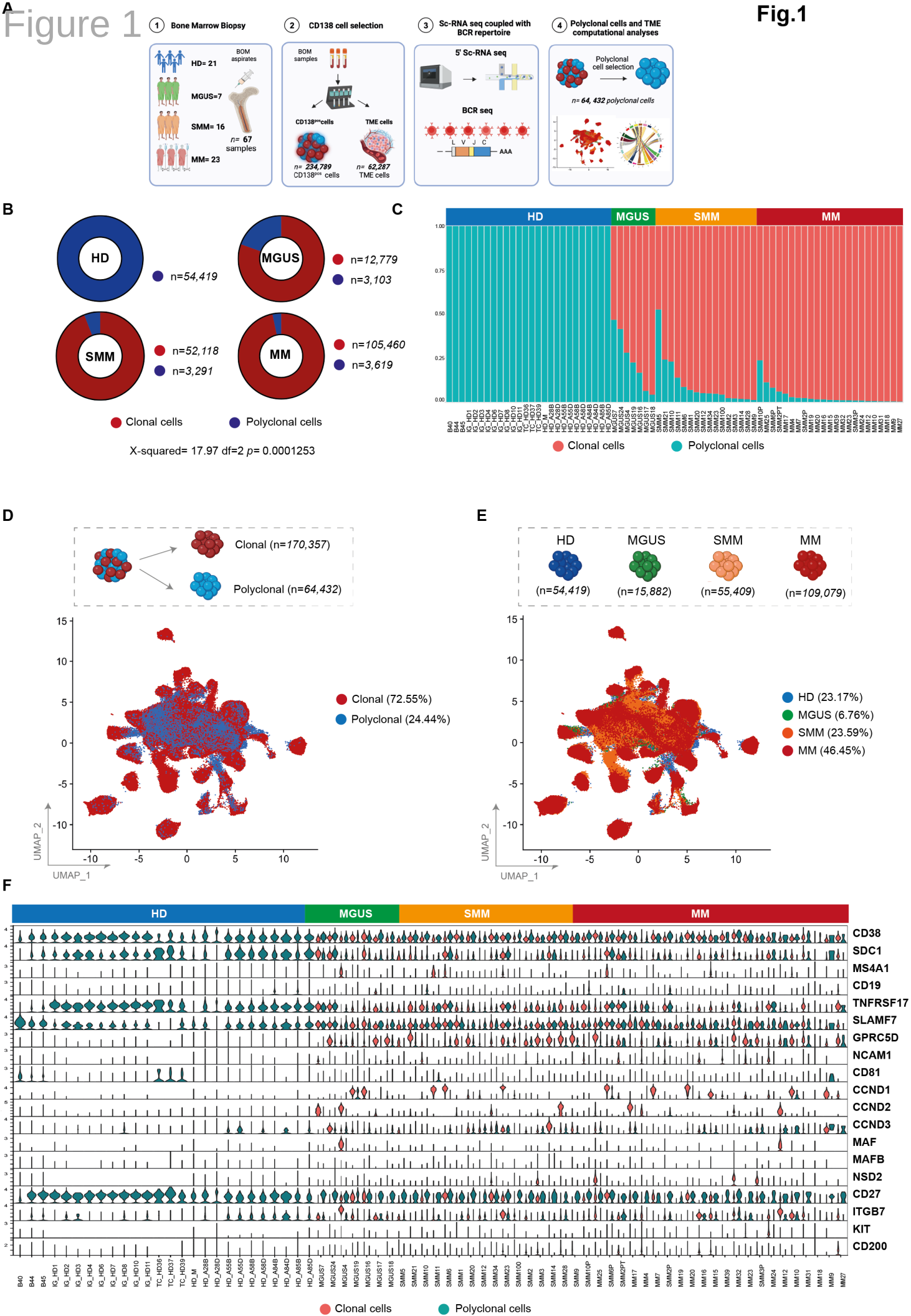

Figure 2

Fig.2

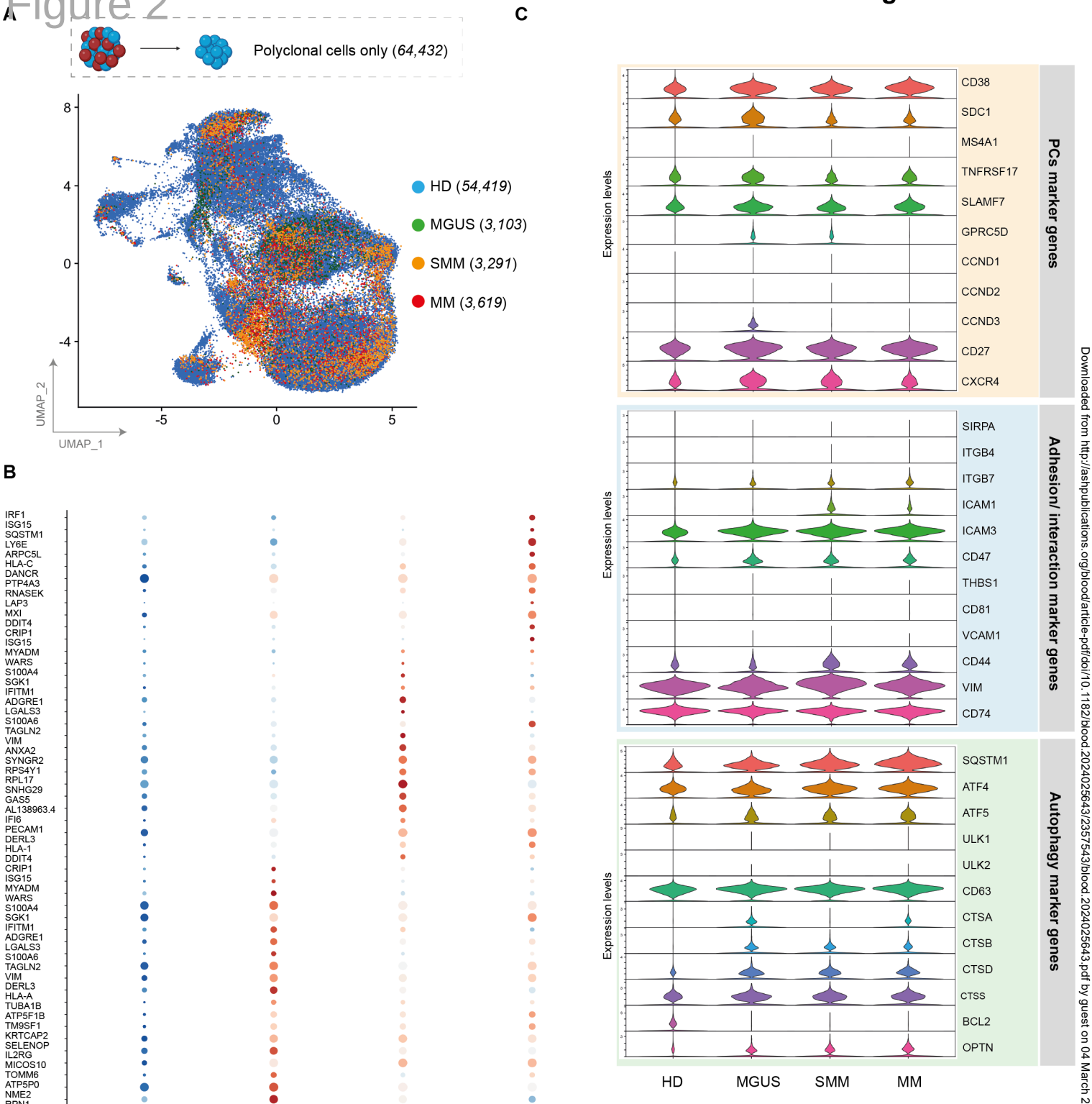

Figure 3

Fig.3

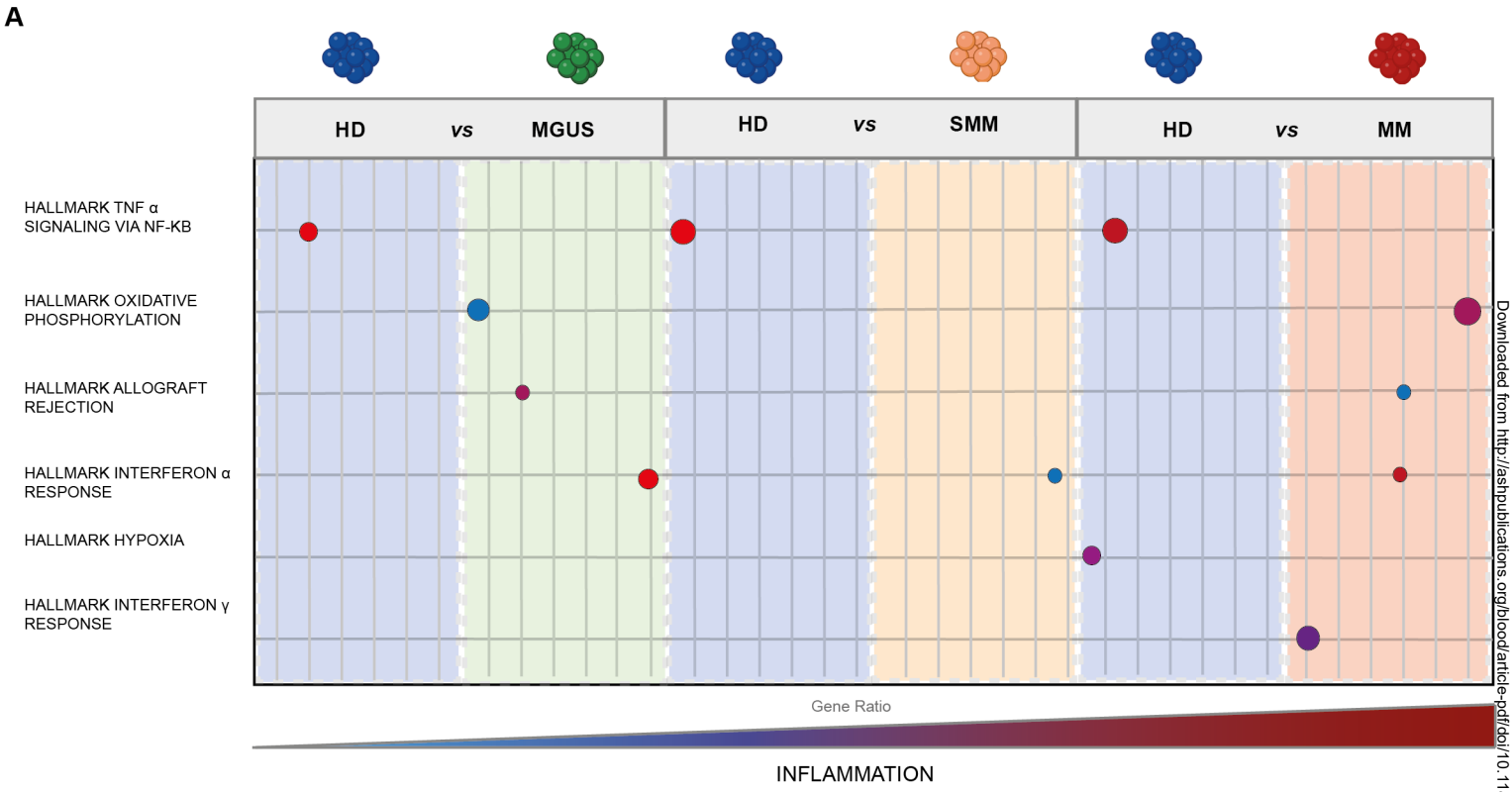

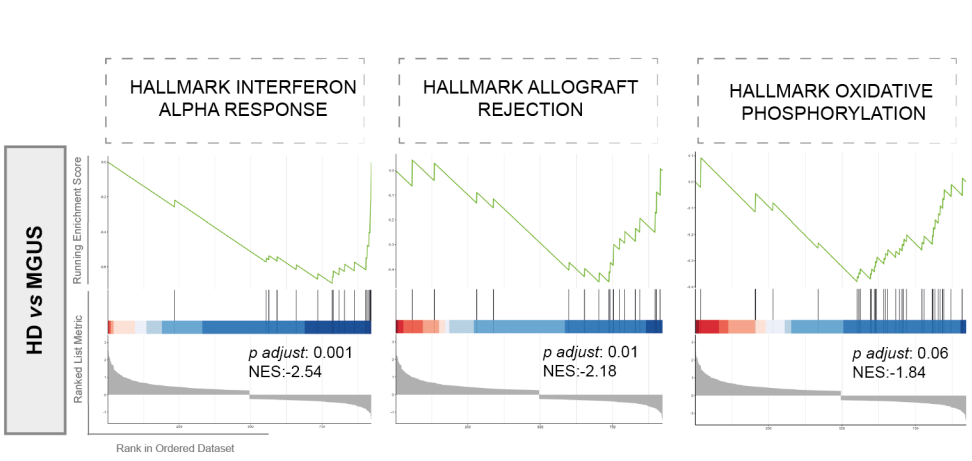

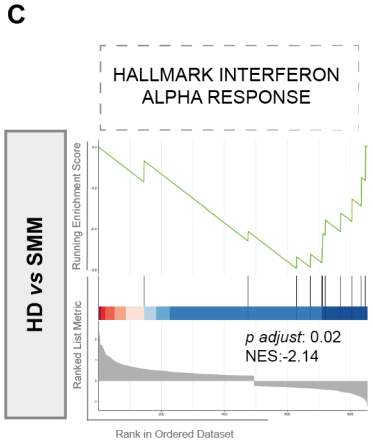

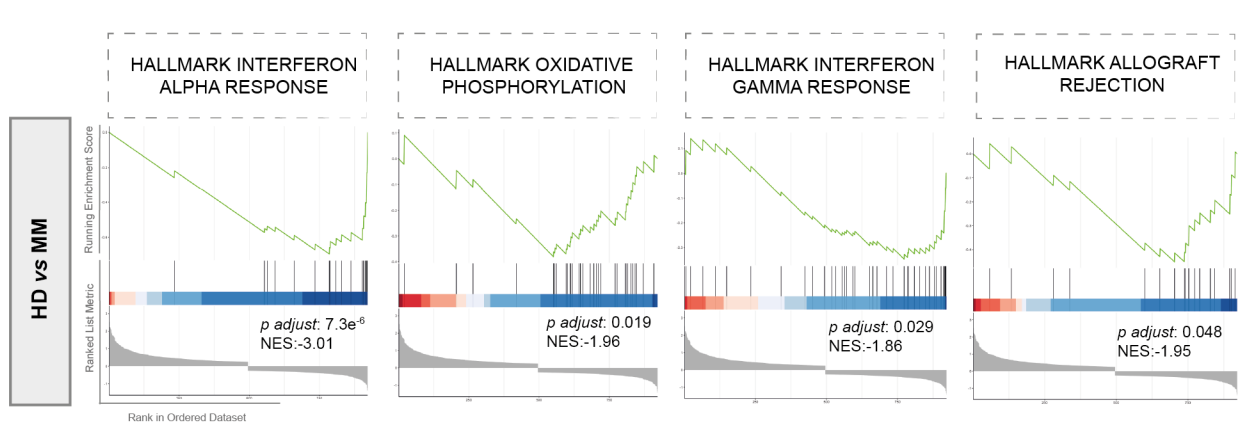

Figure 4

Fig.4

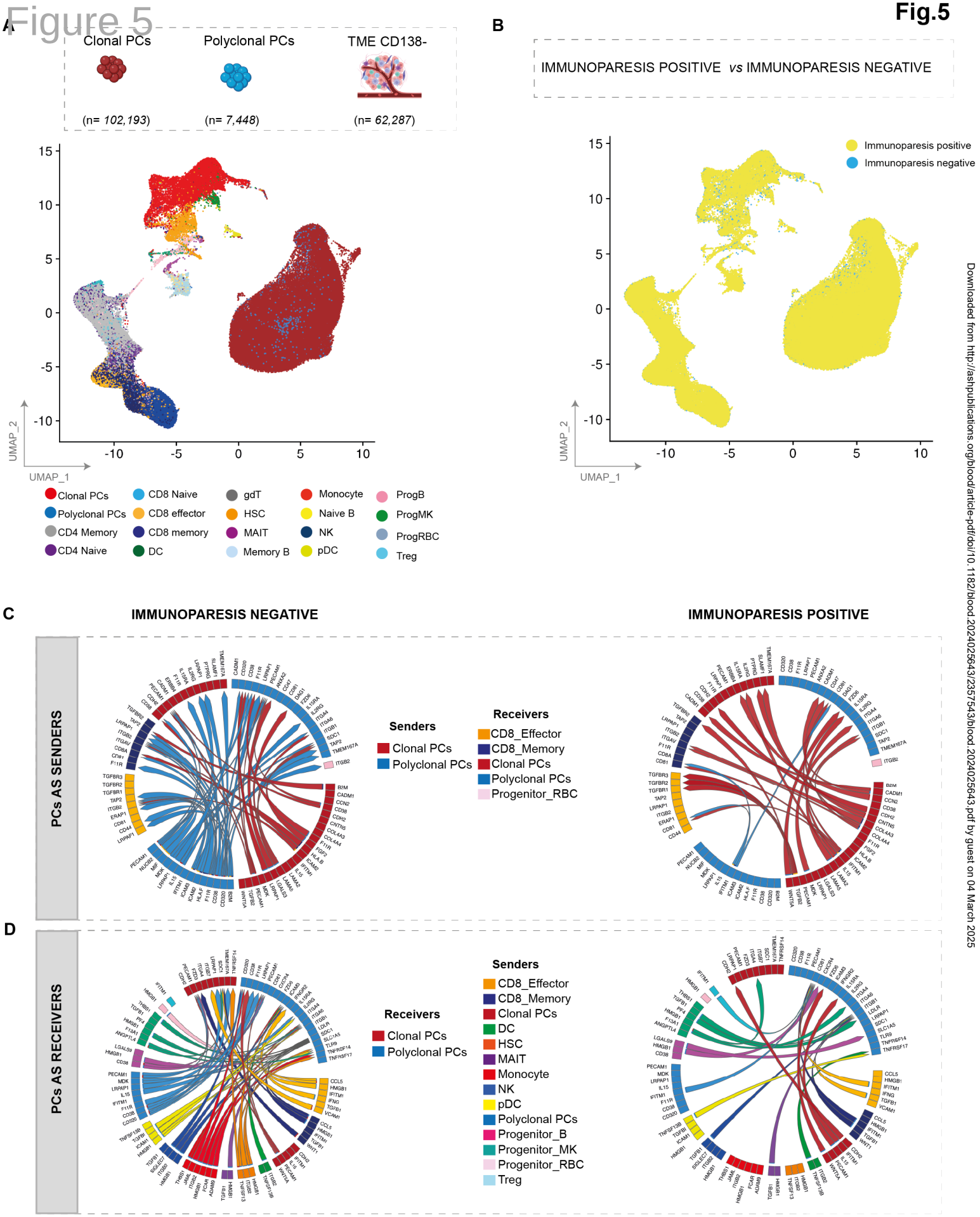

Figure 6

Fig.6

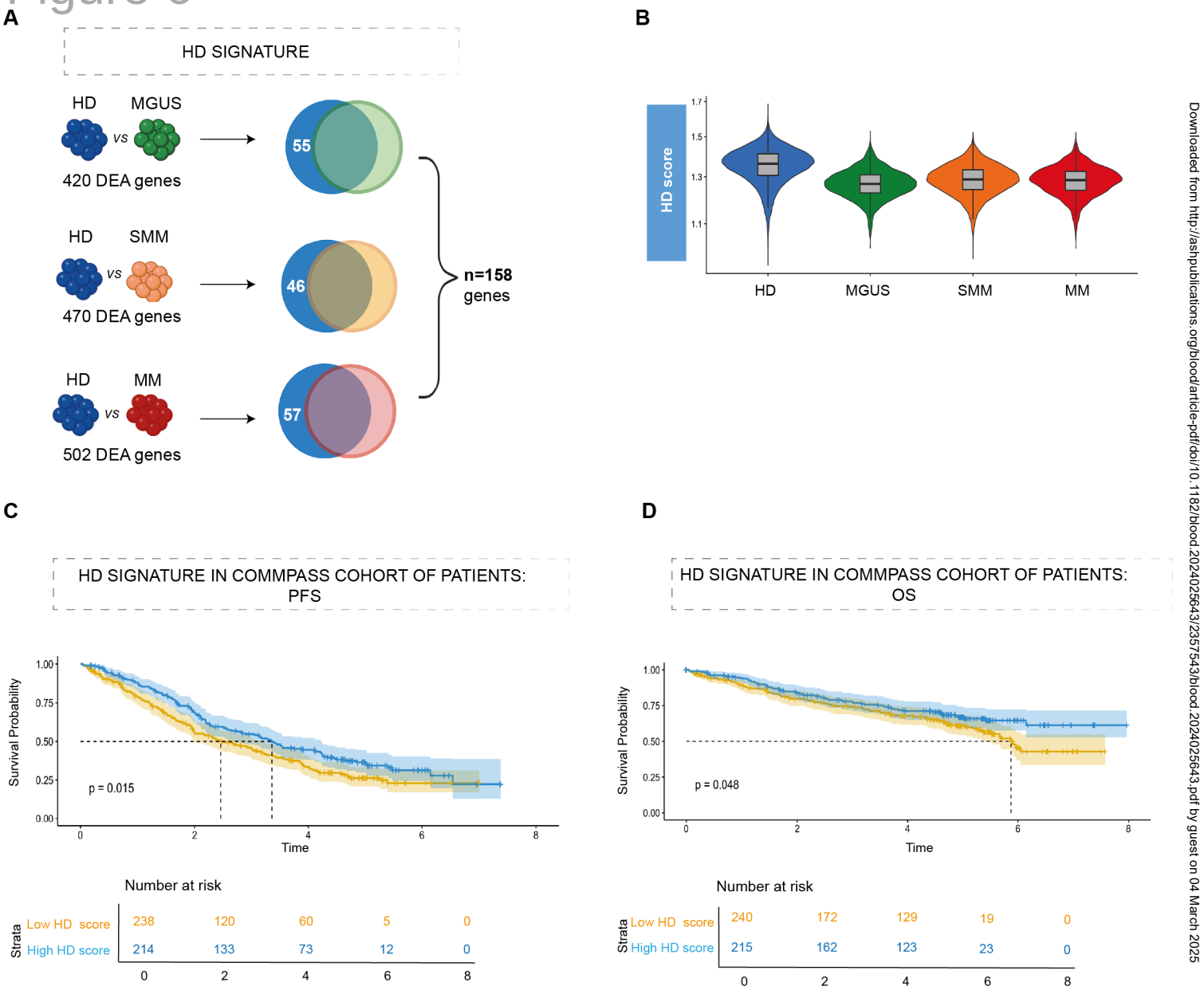

ABERRANT SINGLE-CELL PHENOTYPE AND CLINICAL IMPLICATIONS OF GENOTYPICALLY-DEFINED POLYCLONAL PLASMA CELLS IN MYELOMA

Context of Research

The functional status of genotypically-defined polyclonal plasma cells (pPCs) in monoclonal gammopathies is not known

Aim of This Study

Investigate the role of a disrupted tumor microenvironment (TME) and residual polyclonal PCs (pPCs) in PC dyscrasias

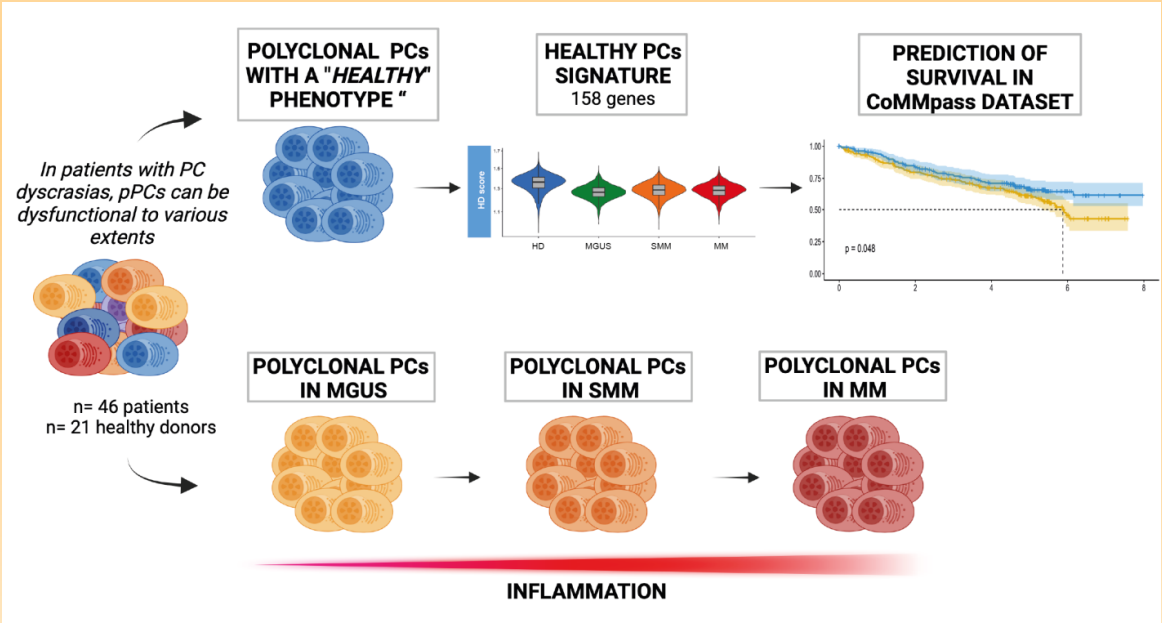

Conclusions: **pPCs in patients with PCs dyscrasias show functional disruption that correlates with an an inflammatory milieu typical of disease pathogenesis and explains cases of immunoparesis seen upon progression. Cases that retain a "healthy" PC signature show improved survival after treatment.**